

NRC Publications Archive Archives des publications du CNRC

Comparative studies of co-conversion of waste activated sludge and lignocellulosic wastes through hydrothermal liquefaction

Nazari, Laleh; Wang, Haoyu; Ray, Madhumita B.; Xu, Chunbao

This publication could be one of several versions: author's original, accepted manuscript or the publisher's version. / La version de cette publication peut être l'une des suivantes : la version prépublication de l'auteur, la version acceptée du manuscrit ou la version de l'éditeur.

For the publisher's version, please access the DOI link below. / Pour consulter la version de l'éditeur, utilisez le lien DOI ci-dessous.

Publisher's version / Version de l'éditeur:

<https://doi.org/10.1016/j.biombioe.2025.107671>

Biomass and Bioenergy, 194, C, 2025-02-05

NRC Publications Archive Record / Notice des Archives des publications du CNRC :

<https://nrc-publications.canada.ca/eng/view/object/?id=109aea98-1906-4d95-a56a-aa37e3dcd39d>

<https://publications-cnrc.canada.ca/fra/voir/objet/?id=109aea98-1906-4d95-a56a-aa37e3dcd39d>

Access and use of this website and the material on it are subject to the Terms and Conditions set forth at

<https://nrc-publications.canada.ca/eng/copyright>

READ THESE TERMS AND CONDITIONS CAREFULLY BEFORE USING THIS WEBSITE.

L'accès à ce site Web et l'utilisation de son contenu sont assujettis aux conditions présentées dans le site

<https://publications-cnrc.canada.ca/fra/droits>

LISEZ CES CONDITIONS ATTENTIVEMENT AVANT D'UTILISER CE SITE WEB.

Questions? Contact the NRC Publications Archive team at

PublicationsArchive-ArchivesPublications@nrc-cnrc.gc.ca. If you wish to email the authors directly, please see the first page of the publication for their contact information.

Vous avez des questions? Nous pouvons vous aider. Pour communiquer directement avec un auteur, consultez la première page de la revue dans laquelle son article a été publié afin de trouver ses coordonnées. Si vous n'arrivez pas à les repérer, communiquez avec nous à PublicationsArchive-ArchivesPublications@nrc-cnrc.gc.ca.



Comparative studies of co-conversion of waste activated sludge and lignocellulosic wastes through hydrothermal liquefaction

Laleh Nazari^a, Haoyu Wang^b, Madhumita B. Ray^b, Chunbao Xu^{c,*}

^a National Research Council of Canada, Aquatic and Crop Resource Development Research Centre, Halifax, Nova Scotia, B3H 3Z1, Canada

^b Department of Chemical & Biochemical Engineering, University of Western Ontario, London, ON, N6A 5B9, Canada

^c School of Energy and Environment, City University of Hong Kong, Hong Kong Special Administrative Region

ARTICLE INFO

Keywords:

Hydrothermal liquefaction
Co-conversion
Waste activated sludge
Lignocellulosic biomass

ABSTRACT

The effects of feedstock type on hydrothermal liquefaction were explored through the co-conversion of waste activated sludge and various lignocellulosic biomass sources, including birchwood sawdust, cornstalk, and waste newspaper. This investigation aimed to produce bio-oil under consistent conditions at 310 °C and a 10-min reaction time, with subsequent comparison to results obtained using single feedstocks. The co-feeding of sludge with cornstalk and sawdust demonstrated the highest bio-oil yields at 34.2 % and 33.7 % wt%, respectively. The comprehensive characterization of the bio-oil products revealed that feedstock type influenced elemental composition and, consequently, the higher heating value of the bio-oils. Bio-oils derived from co-feeds exhibited a significant presence of nitrogenous compounds, esters, and fatty acids in contrast to the high percentage of phenolic compounds found in bio-oils from single feedstocks. Furthermore, these co-feed bio-oils displayed lower molecular weights, higher quantities of low boiling point compounds, increased volatile matter content, and reduced fixed carbon content compared to bio-oils produced from single feedstocks.

1. Introduction

Municipal and industrial wastewater treatment plants generate a substantial volume of waste activated sludge through the biological treatment of wastewater. This sludge poses environmental threats, necessitating additional treatment before disposal or incineration [1]. Sludge handling and management costs may account for up to 70 % of the total wastewater treatment expenses [2]. Consequently, there has been a growing interest in environmentally friendly processes to minimize sludge volume for disposal, replacing conventional methods like landfilling and incineration with the conversion of sludge into bio-energy.

Various options for energy recovery from sludge exist, including biological and thermochemical processes, predominantly resulting in the production of biogas and bio-oil, respectively. Hydrothermal liquefaction (HTL), a thermochemical process developed for energy production from biomass in the presence of water as solvent, eliminates the need for energy-intensive drying in traditional sludge handling processes [3]. Operating at temperatures between 150 and 450 °C under pressures of up to 25–30 MPa, HTL is particularly promising for converting waste biomass with high water content into value-added

products, mainly bio-oil and solid residue (bio-char) in the absence of oxygen. Numerous parameters, such as feedstock type and composition, reaction temperature and time, initial substrate concentration, and the presence of catalysts, significantly influence the yield and composition of liquefaction products.

The type of feedstock plays a crucial role in determining the distribution and composition of products, as major biomass components like lignin, hemicelluloses, and cellulose respond differently to variations in hydrothermal operating conditions [4]. A diverse range of waste feedstocks, including swine manure, cattle manure, microalgae, macroalgae, and municipal wastewater sludge, has been employed in the HTL process, offering substantial waste-disposal benefits and proving cost-effective compared to direct sludge incineration [5,6]. When applied to wastewater sludge, the HTL process also achieves the additional benefit of pathogen reduction, aligning with stringent regulations governing the land application of wastewater sludge.

Early studies, such as Kranich and Eralp (1984), explored sewage sludge liquefaction using hydrogen as a reducing gas and catalysts such as Na₂CO₃, NiCO₃ and Na₂MnO₄. The oil yields were less than 20 wt% with water as the reaction medium [7,8]. In 1986 the STORS process was patented as sludge-to-oil reaction system, operating at 300 °C, 10

* Corresponding author.

E-mail address: chunbaxu@cityu.edu.hk (C. Xu).

<https://doi.org/10.1016/j.biombioe.2025.107671>

Received 27 November 2024; Received in revised form 15 January 2025; Accepted 30 January 2025

Available online 5 February 2025

0961-9534/© 2025 The Authors. Published by Elsevier Ltd. This is an open access article under the CC BY-NC license (<http://creativecommons.org/licenses/by-nc/4.0/>).

MPa and 90 min, producing bio-oil from sludge with oil yields ranging from 10 to 20 wt% and char from 5 to 30 wt% [9,10]. Later, investigations by Malins et al. (2015) demonstrated the influence of various conditions on the HTL process of sewage sludge, including sludge-to-water ratio (1:10–1:15), reaction temperature (200–350 °C), initial H₂ pressure (2.0–11.0 MPa), residence times (10–100 min), and catalyst types (Na₂CO₃, Raney nickel, FeSO₄, MoS₂). The optimal conditions (5.0 MPa H₂ pressure, 300 °C temperature, and 40 min residence time) yielded the highest bio-oil (47.79 wt%). Maintaining a 1:5 sewage sludge-to-water ratio with a 5 wt% FeSO₄ catalyst concentration resulted in bio-oil with the best energy recovery (69.84 %), total conversion (70.64 wt%), and a calorific value of 35.22 MJ/kg [11].

Recent research has expanded comparisons between bio-oil production from HTL of sewage sludge and other waste biomasses such as algae or manure. These studies emphasize the impact of feedstock composition on bio-oil yields and characteristics, providing valuable insights for optimizing the HTL process.

Vardon et al. (2011) investigated feedstock composition effects on hydrothermal liquefaction at 300 °C, 10–12 MPa pressure, and 30 min reaction time using *Spirulina* algae, swine manure, and digested sludge. Organic matter order was *Spirulina* algae > swine manure > digested sludge, correlating with bio-oil yields: 32.6 wt% for algae, 30.2 wt% for manure, and 9.4 wt% for digested sludge. The feedstock type also had a great influence on the boiling point distribution of the bio-oils; algae bio-oil had the highest low boiling point compounds, while sludge bio-oil had the largest fraction of high boiling point compounds [5].

In another work, Huang et al. (2013) explored rice straw, *Spirulina*, and sewage sludge in hydrothermal liquefaction at 350 °C, 9.4–10.1 MPa, and 20 min [12]. Microalgae and sewage sludge are mainly composed of proteins, lipids and carbohydrates while the main components of rice straw are lignin, cellulose and hemicellulose. Sludge yielded the highest bio-oil (39.5 wt%) compared to microalgae (34.5 wt%) and rice straw (21.1 wt%), but had the most solid production (45.7 wt%) and lowest conversion. The feedstock type also affected the composition of the bio-oils. Rice straw bio-oil contained the highest phenolic compounds, while esters dominated bio-oils from both sludge and algae. Obeid et al. (2021) studied different reaction temperatures (250, 300, 350 °C) and times (0–60 min) in hydrothermal liquefaction with three feedstocks: *Tetraselmis* sp. microalgae, sewage sludge, and *Radiata* pine [13]. Microalgae yielded the highest bio-crude oil (up to 30 wt%), followed by sludge (up to 25 wt%) and pine (up to 10 wt%). The presence of inorganic components in the biomass was found to either catalyze or inhibit the formation of bio-crude oil, depending on their composition. Inorganic fractions in the sludge were observed to inhibit the formation of oil, while those in the microalgae appeared to act as catalysts for oil formation.

In a prior study by the authors, the co-conversion of waste activated sludge (WAS) and birchwood sawdust for bio-oil production exhibited advantages, including lower molecular weight (hence less viscosity) compared to bio-oils from individual feedstocks [14]. The operating parameters were optimized through experimental design to achieve maximum bio-oil production, resulting in optimized conditions at 310 °C, 10 min, and 10 wt% substrate concentration. Analyses of the obtained water-soluble product (WSP) using the Bio-methane Potential Test (BMP) highlighted its exceptional anaerobic biodegradability, demonstrating superior rates and extents of biogas production compared to untreated waste activated sludge (WAS) during anaerobic digestion.

This study conducted a thorough examination of the impact of incorporating diverse waste lignocellulosic biomass - such as sawdust, cornstalk, and newspaper - into WAS under the identified optimum operating conditions. Co-conversion of sludge and lignocellulosic biomass enhances the solid content and improves the cost-effectiveness of the process while extracting energy from waste and affecting product yields. This approach utilizes two waste streams, aiding in waste management, and improves efficiency by transforming two renewable resources into sustainable bio-energy products. While previous literature

has explored the co-conversion of certain waste streams, differences in operating conditions and feedstocks render those results incomparable. A more comprehensive investigation into co-feeding studies is necessary for hydrothermal liquefaction (HTL) processes.

The novelties of our HTL treatment process lie in its integration of diverse waste streams, potential synergistic effects, and detailed characterization of bio-oils. Given the critical role of wastewater sludge handling in treatment plants, the primary feedstock in this study was waste activated sludge, supplemented with other waste biomasses as co-feed. This approach aimed to increase solids concentration, enhance process economics, and add value to otherwise discarded byproducts. Additionally, it streamlined waste management efficiency by concurrently converting two waste streams into bio-energy, eliminating the need for expensive sludge drying/dewatering processes.

The study extensively examined the effects of different feedstock mixtures on bio-oil yields and characteristics, employing elemental analysis, oil composition analysis, functional group identification, heating value assessments, thermal stability analysis, and boiling point distribution analysis. The results were systematically compared with those obtained from bio-oils produced using single feedstocks, providing a comprehensive understanding of the impact of feedstock composition on the hydrothermal liquefaction process.

2. Experimental methods

2.1. Materials

Birchwood sawdust was sourced from a local lumber mill in London, Ontario, while cornstalks were obtained from a nearby farm. The raw materials underwent milling to achieve a particle size less than 20 mesh. Local newspapers were soaked in water for 24 h, crushed into pulps using a blender, and subsequently dried at 105 °C for 12 h. The dried pulps were ground with a Wiley Mill into particles <20 mesh and stored for future use. Waste activated sludge (WAS) was collected from the Adelaide Pollution Control Plant in London, Ontario, specifically from rotary drum thickeners, and stored at 4 °C prior to experiments.

The catalyst, potassium hydroxide, was procured from Sigma-Aldrich and used as received. For clarity in subsequent sections, the feedstocks are designated as follows: BS (birchwood sawdust), CS (cornstalk), NP (newspaper), BS-WAS (mixture of birchwood sawdust and WAS), CS-WAS (mixture of cornstalk and WAS), and NP-WAS (mixture of newspaper and WAS). A.C.S. reagent-grade acetone, utilized as a reactor rinsing/washing solvent for product separation, was purchased from Caledon Laboratory Chemicals and used as received.

2.2. Experimental setup

Hydrothermal liquefaction experiments were conducted using a 100 mL stirred reactor (Parr 4590 Micro Benchtop reactor), as illustrated in the schematic diagram available elsewhere [15]. In a standard procedure, an appropriate quantity of sawdust, cornstalk, or newspaper (3.35 g, 3.5 g, and 3.45 g, respectively) was added to 40 g of waste activated sludge (WAS), achieving a dry, ash-free substrate concentration of 10 wt%. The feed mixture, combined with KOH as a homogeneous catalyst at 5 wt% of the substrate on a dry, ash-free basis, was introduced into the reactor. The catalyst was selected based on a prior screening study conducted by the authors [15].

As WAS contained approximately 96 wt% water, no additional water was introduced to the reactants as a solvent. The reactor was sealed, and residual air was purged with nitrogen. Subsequently, the reactor was pressurized to 2 MPa using nitrogen and heated while stirring. Once the reactor temperature reached 310 °C, it was maintained at that temperature for 10 min. The reaction was then halted by quenching the reactor in a water/ice bath.

2.3. Products separation procedure

Following the cooling of the reactor to room temperature, the gas within the reactor was gathered into a 1.0 L gasbag for GC-TCD analysis using an Agilent Micro-GC 3000 (with 120 mL of air injected into the gasbag as an internal standard). Subsequently, the reactor was opened, and the solid/liquid products were extracted and transferred to centrifuge tubes. These tubes underwent centrifugation at 4500 rpm for 10 min and were then vacuum-filtered through pre-weighed 0.45 μm glass fiber filter papers, with the filtrate collected as the WSP.

To ensure thorough cleaning of the reactor, it was rinsed with reagent-grade acetone to eliminate any residual materials, including bio-oils and residual chars adhering to the inner reactor wall. The slurry and rinsing acetone were collected and filtered under vacuum through 1.2 μm glass fiber, separating the water-insoluble solids. The total solid residue underwent rinsing with acetone until the filtrate became colorless. The total solid residue was dried at 105 °C overnight until a constant weight was achieved to determine the yield of solid residue (SR) and biomass conversion. Meanwhile, acetone from the filtrate was evaporated at 50 °C using a rotary evaporator. The resulting dark-colored residue was weighed and designated as bio-oil. Further details regarding yield calculations are outlined elsewhere [15].

2.4. Analysis of products

Elemental analysis of the raw materials and products was performed on a Flash EA 1112 analyzer, employing 2,5-bis (5-tert-butyl-benzoxazol-2-yl) thiophene (BBOT) as the calibration standard; oxygen content was estimated by difference. Heating values were calculated using Dulong's formula ($\text{HHV} = 0.3383\text{C} + 1.422\left(\text{H} - \frac{\text{O}}{8}\right)$) where C, H, and O represent the mass percentages of carbon, hydrogen and oxygen, respectively [16].

Gaseous product compositions were determined through gas chromatography equipped with a thermal conductivity detector (GC-TCD Agilent Micro-GC 3000).

Bio-oil products underwent analysis using a Waters Breeze gel permeation chromatography (GPC-HPLC) instrument (1525 binary pump, UV detector set at 270 nm, Waters Styragel HR1 column at 40 °C) determining average molecular weight and polydispersity index (PDI) with THF as the eluent at a flow rate of 1 ml min⁻¹ and linear polystyrene standards. The average molecular weights of the bio-oils were obtained from the GPC profiles. Additionally, bio-oils were analyzed by gas chromatograph-mass spectrometer [GC-MS, Agilent Technologies, 5977A MSD] with a SHRXI -5MS column (30 m \times 250 μm \times 0.25 μm) with a temperature program of 60 °C (hold for 2 min) \rightarrow 120 °C (10 °C/min) \rightarrow 280 °C (8 °C/min, hold for 5 min)] for identifying the composition of bio-oils. The samples were diluted to 0.5 % (g/g) with acetone and filtered to remove particles before analysis. The 1 μl sample was injected with a split ratio of 10:1. Compounds in the heavy oil were identified by means of the NIST Library with 2011 Update.

Volatile matter (VM) and fixed carbon (FC) contents of the samples were determined by PerkinElmer Pyris 1 Thermal gravimetric analyser (TGA) in a nitrogen and air atmosphere with the gas flow rate of 20 mL/min. The samples were oven dried at 60 °C for an hour before the analysis. They were then heated from 40 °C to 900 °C under N₂ atmosphere with a heating rate of 10 °C/min, and the weight loss (TG) and the rate of weight loss (DTG) of the samples were recorded continuously. The gas was then switched to air and the samples were burned in the air at 900 °C for 20 min to determine their fixed carbon (FC) and ash content.

A total organic carbon (TOC) analyzer (Shimadzu TOC-ASI) was used to measure the total organic carbon content in water soluble products. The moisture content and ash contents were determined based on ASTM E1756-08 (drying the samples at 105 °C for at least 12 h) and ASTM E1755-1 (heating the samples at 575 °C for 3 h), respectively. Physico-

chemical analyses of the sludge including total solids (TS), volatile solids (VS), and chemical oxygen demand (COD) were performed according to the Standard Methods [17]. The Fourier transform infrared spectrometer (FT-IR) analyses were conducted on a PerkinElmer FT-IR spectrometer and the spectra were recorded in the region of 4000-550 cm⁻¹.

The metal composition of the produced ash and biosolids was determined using inductively coupled plasma (ICP-AES). The solid samples underwent an acidic digestion with nitric and sulfuric acid at 90 °C for 1 h. They were then cooled to ambient temperature followed by filtration and dilution prior to ICP analysis. The samples were heated up to 6000- K in order to vaporize and ionize the target metals Na, K, Mg, Ca, Mn, Fe, Zn, Al and Si. The ions were detected and analyzed by atomic emission spectrometry.

The lignocellulosic feedstock (BS, CS, and NP) underwent compositional analysis including lignin, cellulose, and hemicellulose content, using thermogravimetric analysis [18]. Prior to analysis, a 16-h Soxhlet extraction with acetone served as a pre-treatment to eliminate extractives that could potentially interfere with the results. The resulting extractive-free biomass was subjected to the "Klason lignin" determination method which is defined as the insoluble part of biomass in a 72 % sulfuric acid solution.

For cellulose and hemicellulose determination, holocellulose was initially prepared, involving treatment of biomass with an acid solution (sodium acetate acid) at 75 °C for 5 h. Subsequently, α -cellulose extraction was performed, defining it as the residual component of holocellulose insoluble in a 17.5 wt% NaOH solution at room temperature for a 30-min incubation period. The hemicellulose content was then calculated by deducting the corrected cellulose content from the corrected holocellulose content [18].

Finally, the Energy Recovery Ratio (ER) of the bio-oil was calculated and defined as the ratio of energy generated in the form of bio-oil to the initial biomass's energy content:

$$\text{ER (\%)} = \frac{\text{HHV of bio - oil} \times \text{mass of bio - oil}}{\text{HHV of the feed} \times \text{mass of feed}} \times 100$$

3. Results and discussion

3.1. Feedstock characterization

The physicochemical characteristics of the different feedstocks are given in Table 1a. Proximate analysis reveals that birchwood sawdust boasts the highest volatile matter content on a dry weight basis (83.5 %) compared to newspaper (76.1 %), cornstalk (74.1 %), and WAS (62.2 %). The organic matter of lignocellulosic biomass is mostly comprised of lignin, cellulose and hemicelluloses, while wastewater sludge primarily consists of proteins, lipids and carbohydrates. In contrast to volatile matter, sludge exhibits a notably high ash content of 23.6 %, surpassing cornstalk (10.7 %), newspaper (9.2 %), and sawdust (0.23 %). Elemental analysis reveals a higher nitrogen concentration in sludge, likely attributed to protein presence. Proteins, which also contain sulfur, contribute to the presence of sulfur-containing amino acids like methionine and cysteine [19]. Consequently, liquefaction products from sludge could be expected to contain nitrogenous and sulfur compounds resulting from the thermal degradation of proteins. The molar ratio of H/C and O/C in different feedstock ranged from 1.57 to 1.65 and 0.50 to 0.77, respectively, with low high heating values (HHV) of 14.4-16.9 MJ/kg.

The metal contents in the ash were analyzed by ICP-AES and the results are shown in Table 1b. The analysis shows that the primary constituents of the ash fraction are calcium, potassium, and magnesium for lignocellulosic biomass, and iron and calcium for waste activated sludge.

Table 1a
Characteristics of the feedstock.

Parameter	Birchwood sawdust	Cornstalk	Newspaper	WAS
<i>Proximate analysis</i>				
Volatile matter (VM) ^{a,b} (wt%)	83.45	74.08	76.14	62.24
Fixed carbon (FC) ^{a,b} (wt %)	16.32	15.21	14.64	14.09
Ash ^{a,b} (wt%)	0.23	10.71	9.22	23.67
Moisture (wt%)	0 ^c	0 ^c	0 ^c	96.1
pH	–	–	–	7.76
<i>Ultimate analysis^a</i>				
C (wt%)	47.6	42.8	42.1	38.04
H (wt%)	6.3	5.7	5.5	5.23
N (wt%)	0	0.46	0	7.20
S (wt%)	0	0	0	0.75
O ^d (wt%)	45.9	40.3	43.2	25.1
H/C	1.59	1.60	1.57	1.65
N/C	0	0.01	0	0.16
O/C	0.72	0.71	0.77	0.50
HHV ^e (MJ/kg)	16.9	15.4	14.4	15.8

^a On a dry basis.^b Determined by TGA at 900 °C in nitrogen and air atmosphere.^c Raw material was dried in an oven at 105 °C for 24 h before the experiments.^d Calculated by difference (100 % - C% - H% - N% - S%-Ash%).^e Higher Heating Value (HHV) calculated by Dulong formula, i.e., HHV (MJ/kg) = 0.3383C + 1.422(H-O/8).**Table 1b**
Concentration of major inorganic elements in ash detected by ICP-AES.

	Sawdust (wt %)	Cornstalk (wt %)	Newspaper (wt %)	WAS (wt %)
Aluminum (Al)	0.76	0.51	2.39	0.75
Barium (Ba)	0.02	0.01	0.01	0.09
Calcium (Ca)	13.27	8.11	21.81	9.87
Chromium (Cr)	Nd	0.02	Nd	0.03
Copper (Cu)	0.02	0.01	0.04	0.23
Iron (Fe)	0.68	0.65	0.19	25.36
Potassium (K)	12.19	19.61	0.06	2.18
Magnesium (Mg)	2.74	2.34	0.53	1.47
Manganese (Mn)	0.43	0.04	Nd	0.25
Sodium (Na)	2.01	0.26	1.37	2.91
Nickel (Ni)	Nd	0.01	Nd	Nd
Silicon (Si)	0.07	0.03	0.04	1.21
Zinc (Zn)	0.19	0.03	0.01	0.16

Nd: Not detected.

3.2. Products distribution

Table 2 provides the yields of products, conversion percentages, and molecular weights of bio-oils. Gaseous product yields, all below 1 wt%, are not discussed further; Micro-GC analysis revealed carbon dioxide as the major component with traces of hydrogen and ethylene.

Table 2
Distribution of products and molecular weight of the bio-oils from HTL of different feedstocks at 310 °C, 10 min and 10 wt% solid concentration.

Feedstock	Oil yield (wt%)		Solid yield (wt%)	WSP yield (wt%)	Conversion (wt%)	MW (g/mol)
	Experimental	Theoretical				
BS-WAS	33.7 ± 0.3	35.03	15.5 ± 0.1	50.7 ± 0.2	84.5 ± 0.1	535
CS-WAS	34.2 ± 2.3	25.26	6.4 ± 1.1	59.4 ± 1.3	93.6 ± 1.1	448
NP-WAS	28.8 ± 0.6	37.96	10.3 ± 0.1	60.9 ± 0.7	89.7 ± 0.1	562
WAS	23.1 ± 3.8	–	13.2 ± 1.7	63.7 ± 5.5	86.8 ± 1.7	415
BS ^a	39.5 ± 2.8	–	12.0 ± 1.2	48.2 ± 3.9	87.9 ± 1.2	856
CS	26.08	–	10.72	63.20	89.28	451
NP	43.58	–	13.72	42.70	86.28	615

^a Results taken from a previous study by the authors [15] (at 300 °C, 30 min and 10 wt% solid concentration).

Comparing co-feed experiments, BS-WAS and CS-WAS generated the highest bio-oil yields, with CS-WAS resulting in the least solid residue and the highest conversion rate. Generally, the conversion extent under HTL conditions follows the order: lipids > proteins > carbohydrates [20]. Low carbohydrate conversion is attributed to higher hemicellulose and lignin contents. Notably, Table 3's compositional analysis shows that newspaper has the highest lignin content among feedstocks, potentially contributing to lower bio-oil yield for NP-WAS. The higher lignin content of newspaper compared to cornstalk and sawdust aligns with previous findings [21–26]. This is also confirmed by TGA analysis of the feedstock which will be discussed later in the next sections.

CS-WAS's high conversion may stem from cornstalk's lower lignin content compared to other lignocellulosic biomass. Research indicates that hydrothermal processing of lignin increases solid production due to subsequent depolymerization and re-polymerization or self-condensation [27]. Similar results were reported by Zhang et al. for co-liquefaction of waste newspaper and pulp/paper-mill sludge, where bio-oil yield was 31.2 wt% with 15.6 wt% solid residue at 300 °C, 20 min, 11.3 wt% solid concentration, and 5 wt% KOH catalyst [26].

The enhanced conversion in CS-WAS could be ascribed to the abundant potassium content in CS ash, which may act as a catalyst. This catalytic role of ash aligns with previous findings by Shah et al. (2022) and Xu et al. (2019) [28,29]. Presence of potassium is shown to be effective for suppressing solid yields during hydrothermal liquefaction. It was reported earlier that potassium carbonate can result in reduced solid residue while potassium hydroxide promotes water-gas shift reaction [30,31]. Bhaskar et al. achieved a remarkable conversion of nearly 96 wt% using 0.5 M K₂CO₃ in hydrothermal liquefaction of woody biomass at 280 °C for 15 min [32]. Bi et al. explored the hydrothermal liquefaction of pretreated sorghum bagasse with various catalysts, identifying K₂CO₃ as the most effective, leading to the highest biocrude yield of 61.8 %, with an HHV of 33.1 MJ/kg and low nitrogen and sulfur content [33]. While sodium salts can increase bio-oil yield and inhibit char formation, their activity is generally less than that of potassium salts [34]. In a study by Jindal et al., the overall conversion rate followed the order: K₂CO₃ > KOH > Na₂CO₃ > NaOH [35]. Minor elements such as Fe or Ni may have also contributed to the reduced solid yields observed in the mixture of cornstalk and WAS.

The oil yields obtained from the liquefaction of individual feedstocks (WAS, BS, CS and NP) detailed in Table 2 for reference. To assess the impact of co-feeding, the ratio of lignocellulosic feedstock to WAS, and

Table 3
Composition of different lignocellulosic biomass feedstock.

	Lignin ^a	Cellulose ^b	Hemicellulose ^c
Newspaper (NP)	26.3 ± 0.3	34.6 ± 0.2	33.8 ± 0.1
Birchwood sawdust (BS)	23.4 ± 0.1	31.8 ± 0.1	28.4 ± 0.2
Cornstalk (CS)	17.7 ± 0.1	37.6 ± 0.2	33.5 ± 0.2

^a Klason lignin (acid soluble).^b Alpha-cellulose.^c By difference.

considering the rule of mixtures, theoretical yields from co-feeds are calculated and presented in Table 2. A comparative analysis of the experimental and theoretical yields underscores the significant influence of the feedstock type on co-feeding outcomes. For instance, in the BS-WAS sample, the yields are nearly identical, suggesting that the addition of sawdust to WAS has no synergistic effect on oil yield. In contrast, the CS-WAS sample demonstrates an improvement in oil yield compared to the theoretical yield, possibly attributed to the catalytic effect of potassium in CS ash. Conversely, NP-WAS exhibits a decrease in oil yield compared to the theoretical yield, suggesting detrimental effects on co-liquefaction, potentially stemming from the high lignin content of NP.

The molecular weights of the bio-oils, as detailed in Table 2, were determined via GPC and ranged from 448 to 562 g/mol, with the lowest recorded molecular weight of 448 g/mol observed for the CS-WAS bio-oil. Comparative molecular weights of bio-oils derived from single feedstocks are also provided for reference. A notable observation is that the introduction of additional lignocellulosic biomass, such as sawdust, cornstalk, or MSW, as a co-feed to wastewater sludge results in bio-oils with lower molecular weights and, consequently, lower viscosity compared to those produced solely from lignocellulosic biomass. For instance, the molecular weight of the bio-oil from BS (856 g/mol) experienced a significant reduction when BS was co-liquefied with WAS, yielding a molecular weight of 535 g/mol for BS-WAS. Notably, the CS-WAS sample exhibits the least impact of co-feeds on its molecular weight. This trend is visually represented in Fig. 1, illustrating the molecular weight distribution of bio-oils produced from single feedstocks and co-feeding. Fig. 1 indicates higher proportions of low-molecular-weight compounds in bio-oils derived from co-feeds compared to those obtained from single lignocellulosic biomass.

3.3. Elemental analysis and higher heating value

The elemental analysis of bio-oils and solid residues resulting from various co-feeds, along with their higher heating values (HHV), is presented in Table 4. Notably, the carbon contents of the bio-oils (69.1–72.4 %) exhibited a substantial increase compared to the original biomass materials (38.0–47.6 %). Furthermore, the oxygen contents of the oils (16.3–22.1 %) were significantly lower than those in the feedstocks (25.1–45.9 %), leading to elevated higher heating values of the oils. The bio-oils showcased HHVs ranging from 26.4 to 32.0 MJ/kg, in stark contrast to the 14.4–16.9 MJ/kg recorded for the raw feedstocks.

The Van Krevelen diagram (Fig. 2) elucidates the molar H/C and O/C ratios, offering insights into the impact of different feedstock types on the elemental composition of the products. While BS-WAS and NP-WAS

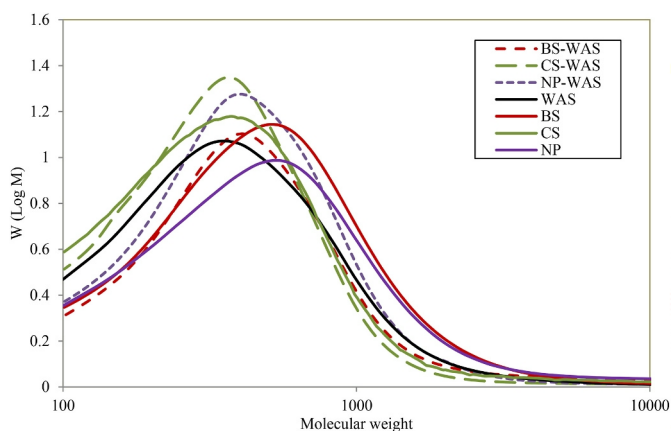


Fig. 1. Normalized molecular weight distribution of the bio-oils (dashed lines represent the experiments with co-feeding and solid lines represent the experiments with single feedstock).

exhibited similar elemental compositions and, consequently, similar higher heating values, the bio-oil from CS-WAS displayed higher oxygen and lower hydrogen content, resulting in a lower HHV. Generally, the H/C molar ratio of the oils (0.85–1.26) decreased compared to the initial H/C ratio of the feedstock (1.57–1.65). This reduction in H/C molar ratio signifies the dehydrogenation of alcohols and amines, leading to the production of aldehydes, ketones, and carboxylic acid derivatives. A lower H/C molar ratio also indicates a higher prevalence of unsaturated compounds in the bio-oils.

The O/C ratio for all of the produced oils (0.17–0.24) was much lower than that of the biomass feed (0.50–0.75 from Table 1a), suggesting occurrence of deoxygenation reactions (dehydration and/or decarboxylation) of the intermediates. This ultimately results in the production of water-soluble products (WSP) and CO₂ [36]. Significant amounts of water (50–60 wt%) were formed as the WSP as presented in Table 2. Micro-GC analysis indicated that the main component of the gas product was CO₂. This implies that oxygen in biomass is predominantly removed in the form of CO₂ and WSP during the liquefaction process. In a prior work by the authors, the Bio-methane Potential (BMP) test of the WSP from BS-WAS demonstrated rapid initial methane production (no lag phase), peaking at around 800 mL per g VS added after 31 days. This suggests that a considerable amount of biogas can be produced from this by-product, rendering the co-production of biogas and bio-oil feasible [14].

The elemental compositions of bio-oils and solid residues derived from single feedstocks of BS and WAS are also presented in Table 4 and Fig. 2 for comparative analysis. The incorporation of WAS, characterized by higher carbon and hydrogen content and lower oxygen content, enhanced the quality of bio-oil obtained through co-feeding. The H/C molar ratio of 1.1 in the BS-derived bio-oil suggests the presence of aromatic compounds, contributing to higher viscosity. However, co-feeding (BS-WAS) resulted in a reduction of aromatic compounds, reflected in an increased H/C ratio. The O/C ratios of BS-WAS bio-oil fall between those of bio-oils from WAS and BS, notably decreasing compared to BS-derived bio-oil. Another notable difference lies in the higher nitrogen concentration and the presence of sulfur in bio-oils from co-feeds with WAS, attributable to the elevated sulfur and nitrogen levels in WAS relative to other feedstocks. WAS's high protein content contributes to higher nitrogen levels (3.1–3.6 %) compared to the minimal nitrogen content in bio-oil from sawdust (0.1 %). Although the sulfur content in these bio-oils is relatively low compared to many petroleum crudes (0.1 %–3 %), their nitrogen and oxygen contents remain higher than those found in petroleum oil, which typically has 0.05–1.5 % oxygen and 0.01–0.7 % nitrogen. Further upgrading processes would be required to enhance the quality of these bio-oils.

The elemental composition of solid residues reveals that the hydrogen content of chars resulting from co-feeds ranged from 2.2 % to 3.9 %, while carbon predominantly existed as coke, constituting 25.3 %–50.7 % of the composition. The H/C molar ratio of the chars, ranging from 0.92 to 1.1, signifies the prevalence of aromatic compounds. Additionally, oxygen was primarily present in the ash components, forming metal oxides that remained inactive throughout the process. A comparison with solid residue from the sawdust experiment highlights higher H/C values and significantly lower oxygen content in the co-feeds' solid residues. However, despite these differences, the heating values were lower due to the elevated ash content in the solid residues from the co-feeds. While these solid residues could serve as an energy source for other plant operations, it is crucial to remove the ash before utilizing them as solid fuels for heat generation. High ash content can lead to severe corrosion issues, as ash remains as a residue after incineration.

ICP-AES analysis of biochar from BS-WAS revealed its composition, containing 4.1 wt% Ca, 1.3 wt% Fe, 0.3 wt% Mg, 1.8 wt% K, 1.23 wt% Na, and 0.3 wt% P, along with trace amounts (<0.1 wt%) of Al, Mn, and Si. These bio-chars exhibit potential applications as soil fertilizers, conditioners, or sorbents for both organic and inorganic contaminants in

Table 4
Elemental composition of bio-oils and solid residues obtained from HTL.

Feedstock	Bio-oils								Solid residues					
	C (%)	H (%)	N (%)	S (%)	O (%) ^a	H/C (-)	O/C (-)	HHV (MJ/kg) ^b	C (%)	H (%)	N (%)	S (%)	H/C (-)	O and metal elements (%) ^a
BS-WAS	72.1	7.5	3.1	0.1	17.0	1.25	0.18	32.0	50.7	3.9	2.6	0.1	0.92	42.7
CS-WAS	69.1	4.9	3.6	0.1	22.1	0.85	0.24	26.4	25.3	2.2	1.8	0	1.04	71.6
NP-WAS	72.4	7.6	3.4	0.2	16.3	1.26	0.17	32.4	33.9	3.1	1.8	0	1.10	62.3
BS ^c	66.5	6.1	0.1	0	27.3	1.10	0.31	26.3	69.8	4.5	0.2	0	0.77	25.5
WAS	76.3	9.3	5.5	0.4	7.8	1.46	0.08	37.7	18.8	2.1	1.7	0.1	1.34	77.3

^a Calculated by difference (100 % - C% - H% - N% - Ash%) assuming negligible sulfur content.

^b Higher Heating Value (HHV) calculated by Dulong formula, i.e., $HHV (MJ/kg) = 0.3383C + 1.422(H-O/8)$.

^c Results taken from previous study by the authors at almost the same operating conditions (300 °C, 30 min and 10 wt% solid concentration).

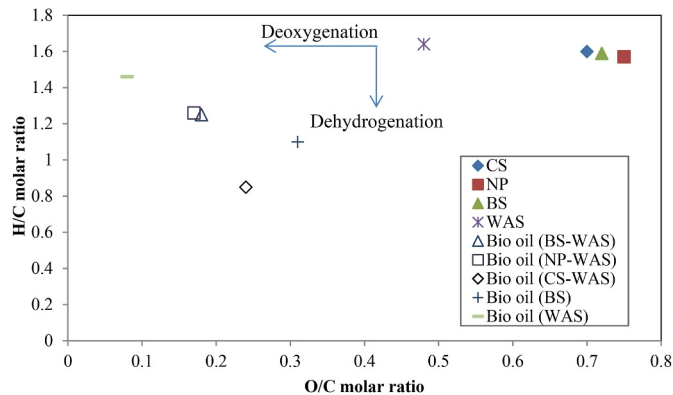


Fig. 2. The Van Krevelen diagram of feedstocks and bio-oils.

soil and water, aligning with previous studies [37–41].

For a comprehensive understanding of carbon distribution in the products, a material balance was conducted, as outlined in Table 5. Elemental analysis determined the carbon composition of bio-oils and solid residues, while total organic carbon (TOC) and Micro-GC analysis provided the carbon content of the WSP and gas products, respectively. Carbon recovery, calculated based on the total % mass of carbon in the products relative to the mass of carbon in dried feedstock, ranged from 89 % to 99 %, showcasing efficient carbon utilization.

The majority of carbon in the feedstock was successfully transferred to the bio-oil, with a smaller portion ending up in the WSP. Only a minimal fraction, particularly notable in the case of CS-WAS, was directed to the solid phase. The highest carbon recovery (99.66 %) was achieved with BS-WAS. Lower mass balances in some cases could be attributed to the loss of certain low boiling point compounds, consistent with findings in the literature [42,43].

3.4. Effect of feedstock type on bio-crude oils functional groups

FT-IR analysis within the range of 4000–550 cm^{-1} was conducted on bio-oils to identify the functional groups and the outcomes are depicted in Fig. 3. Irrespective of the biomass source, all bio-oils exhibited similar functional groups, with variations observed primarily in peak intensities. The broad absorption at 3350 cm^{-1} signifies O-H stretching, indicative of alcohols, phenols, carboxylic acids, and water residues within the bio-oil. Additionally, this peak is attributed to the N-H stretch

Table 5
Carbon distribution in the bio-oil products from liquefaction.

Sample name	Oil (%)	Solid (%)	WSP (%)	Gas (%)	Total C (%)
BS-WAS	54.03	17.54	28.07	0.01	99.66
CS-WAS	56.92	3.91	35.99	0.03	96.86
NP-WAS	50.82	8.54	30.34	0.03	89.74

of protein groups. The bands between 3000 and 2840 cm^{-1} denote C-H stretching vibrations, highlighting the presence of alkyl C-H. The intensities of these peaks in the bio-oils with co-feeds surpassed those from sawdust, suggesting a higher abundance of alkyl groups in the former. The absorbance at 1700 cm^{-1} corresponds to the C=O stretching vibration of carbonyl groups, indicating the presence of ketones, aldehydes, and carboxylic acids in the oils. Peaks at 1611 cm^{-1} , 1516 cm^{-1} and 1456 cm^{-1} represent aromatic ring and its derivatives. The intensity of these peaks, particularly at 1611 cm^{-1} and 1516 cm^{-1} is more pronounced in the oil from BS, suggesting a higher concentration of these compounds. The bands between 1280 and 1000 cm^{-1} can be attributed to C-O vibrations suggesting the possible presence of acids, phenols or alcohols in the bio-oil. Furthermore, absorptions at 1370 and 1456 cm^{-1} are associated with methyl (-CH₃) and methylene (-CH₂) groups, respectively.

3.5. Effect of feedstock type on bio-oils chemical composition

The chemical compositions of bio-oil products were elucidated through GC-MS analysis, and a comprehensive breakdown is provided in Table S1 within the supplementary material. It is essential to acknowledge that due to the high molecular weights and boiling points of certain products generated during hydrothermal liquefaction (HTL), only a fraction is identifiable by GC-MS. Additionally, the solvent peak or losses during the acetone evaporation step in the separation process may mask some low boiling point compounds [44].

The major constituents of the bio-oils from BS-WAS and NP-WAS predominantly included nitrogenous compounds, fatty acids, and phenols. In contrast, the bio-oil from CS-WAS was characterized by esters as the primary fraction, followed by fatty acids and nitrogenous compounds. Other identified components encompass alkanes, alcohols, amines, amide, benzene compounds, and ketones. Phenolic compounds, such as 2-methoxy-phenol and 4-ethyl-2-methoxy-phenol, were more abundant in BS-WAS bio-oil, resulting from the degradation of lignin through aryl ether linkage cleavage. These compounds can also originate from carbohydrates and proteins [12]. Given that cornstarch had lower lignin content than sawdust and newspaper, the CS-WAS bio-oil exhibited the lowest phenolic compound content [45–49]. The presence of nitrogenous compounds, including 1-dodecamine, 2-methylpropanamide, and 1-acetyl-4-[1-piperidyl]-2-butyne, indicates protein degradation through decarboxylation and amino acid rearrangement. Nitrogen-containing organic compounds may engage in the Maillard reaction with sugars, forming pyridines, as evidenced by the presence of pyridine in the bio-oils [50]. Esters dominated the composition of the CS-WAS oil, potentially arising from the decomposition of furan derivatives originating from cellulose breakdown. All bio-oils exhibited a substantial fraction of fatty acids, resulting from lipid decomposition in WAS.

Comparing bio-oils produced from the mixture of WAS and lignocellulosic biomass with those from sawdust, the former displayed lower phenolic compounds, significantly higher ester amounts than oils from

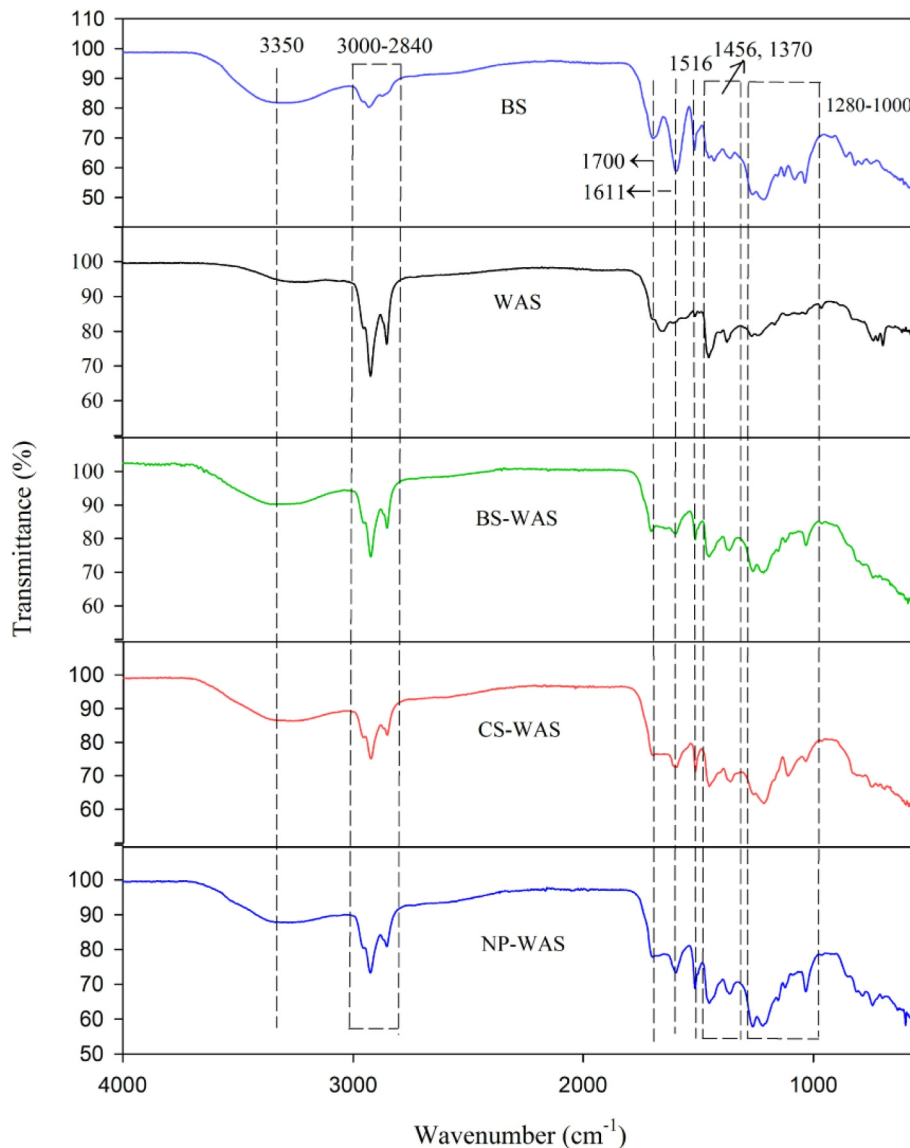


Fig. 3. FT-IR spectra of bio-oils produced from co-liquefaction of WAS and lignocellulosic biomass.

sawdust or WAS alone, and a notably higher percentage of fatty acids, nitrogenous compounds, and saturated compounds than sawdust alone. This trend aligns with findings reported by Huang et al. [12] or bio-oils produced from sewage sludge and rice straw. Their study indicated that the sewage sludge-derived bio-oil had fewer phenolic compounds and a higher percentage of acids, esters, and nitrogenous compounds, attributed to the lower lignin content of sewage sludge. Although benzene and its derivatives in oils produced with WAS were relatively low, they surpassed the levels found in sawdust bio-oil. This suggests that the $-OH$ groups of phenols were more readily removed in reactions involving the mixture of WAS and lignocellulosic biomass. The total percentage of aromatics, including benzene derivatives, phenols, and benzaldehyde, was notably higher in the oil produced with BS compared to co-feeds, corroborating observations in FT-IR analysis.

3.6. Thermal gravimetric analysis

3.6.1. Thermal gravimetric analysis of the feedstocks

The TG and DTG curves depicting the thermal characteristics of various feedstocks are illustrated in Fig. 4. All three lignocellulosic biomass feedstocks exhibited similar decomposition curves (TG), showcasing greater weight loss in the case of BS due to its higher volatile

matter content. However, discernible distinctions were observed when comparing these curves to the TG graph representing WAS. The variation between the sludge profile and the lignocellulosic biomass profiles can be attributed to the distinct organic and inorganic matter characteristics inherent to each. It is well-established that biomass materials predominantly comprise proteins, carbohydrates, lignin, and lipids. As previously noted, sludge primarily consists of proteins, lipids, and carbohydrates, whereas lignocellulosic biomass is chiefly composed of carbohydrates and lignin. The hemicellulose structure of BS, NP, and CS initiated decomposition around $280\text{--}300\text{ }^{\circ}\text{C}$, followed by cellulose degradation at $300\text{--}400\text{ }^{\circ}\text{C}$. In contrast, the decomposition of WAS commenced at approximately $200\text{ }^{\circ}\text{C}$, indicating a temperature range $80\text{--}100\text{ }^{\circ}\text{C}$ lower than that of lignocellulosic biomass. This discrepancy is underscored by the gentler slope in the decomposition curve, highlighting the comparatively reduced levels of volatile matter in WAS. Furthermore, the decomposition curve of WAS exhibited two distinct phases: the first phase ($200\text{--}370\text{ }^{\circ}\text{C}$) attributable to the presence of biodegradable matters and organic polymers in the cells, and the second phase ($370\text{--}500\text{ }^{\circ}\text{C}$) corresponding to non-biodegradable organics such as cellulose and similar materials. The TGA profile consistency between lignocellulosic biomass and sewage sludge aligns with findings reported by other researchers [51–55].

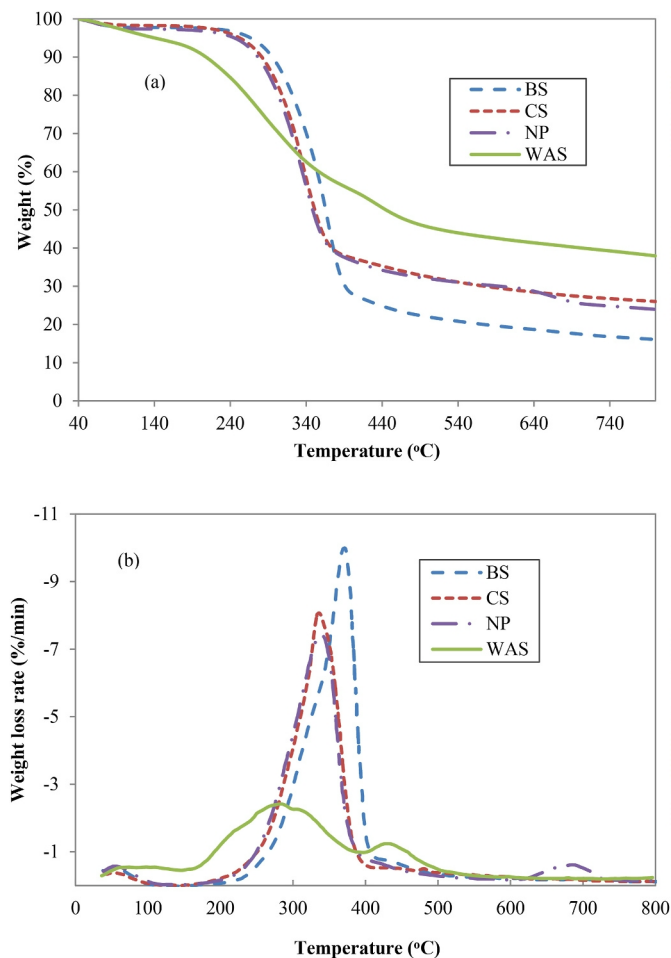


Fig. 4. TGA (a) and DTG (b) curves for the feedstocks.

The distinct thermal decomposition characteristics of various feedstock types are evident in the shapes of the DTG curves. A subtle peak in weight loss around 100 °C is ascribed to moisture dehydration and the release of light volatile compounds in the samples. For lignocellulosic feedstocks, the maximum degradation rate occurs at 330–370 °C, indicative of cellulose decomposition predominating the sample. Signs of lignin are apparent through smaller DTG peaks between 450–500 °C and 620–730 °C, acknowledging lignin's greater stability and broader degradation temperature range of 280–500 °C and 175–800 °C [53]. According to DTG, NP exhibited a higher lignin content compared to CS or BS, validating the compositional analysis detailed in Table 3. The decomposition of WAS unfolds in two distinct stages: the initial phase (200–370 °C) involves the thermal decomposition of proteins and hemicellulose, while the subsequent phase (370–500 °C) entails the thermal decomposition of protein and cellulose. The peak intensities signify that WAS possesses substantially lower cellulose and hemicellulose content compared to lignocellulosic biomass.

3.6.2. Thermal gravimetric analysis of the bio-oils

The TG and DTG graphs illustrating the characteristics of the oils are depicted in Figs. 5 and 6, respectively. Key parameters extracted from the TG/DTG curves, encompassing initial decomposition, final decomposition, peak temperatures, as well as volatile matter (VM) and fixed carbon (FC) contents, are presented in Table 6. Analysis of the TG graph revealed a lack of significant variance in thermal stability among the bio-oils derived from the co-feeds. However, the decomposition of these bio-oils occurred at lower temperatures (161–168 °C) compared to the bio-oil sourced from BS (212 °C). This outcome suggests their

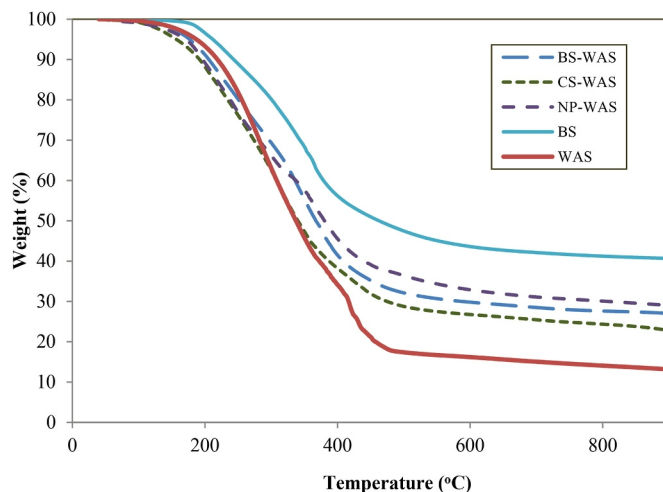


Fig. 5. TGA curves for the bio-oils.

diminished thermal stability, necessitating lower activation energy for decomposition - a characteristic attributed to the lower lignin content in these oils compared to the BS-derived oil. Furthermore, these bio-oils exhibited higher volatile matter content (71–77 %) and lower fixed carbon content (22–28 %) in contrast to the oil produced from BS, which boasts 59.3 % VM and 40.7 % FC. The oil from WAS demonstrated an exceptionally high VM content (86.9 %). This augmented VM content in the bio-oils from mixtures is attributed to the synergistic influence of WAS and lignocellulosic biomass.

The DTG curve is segmented into distinct stages, each corresponding to specific rates of weight loss. In stage "A," the curve reflects the dehydration of superficial moisture and the vaporization of light components. Stage "B" captures the volatilization and vaporization of low molecular weight material, while stage "C" signifies polymerization and dehydration. The concluding stage, "D," represents the char decomposition phase. The delineation of these stages and their respective temperature ranges is illustrated in Fig. 6a–c.

Given the prior oven drying of the oils before TGA, stage A exhibited a minor peak. For BS-WAS and CS-WAS, there was a broader temperature range for the volatilization of low molecular weight material, commencing at 100 °C and concluding at 250–300 °C. Stages B and C for BS-WAS and CS-WAS exhibited more pronounced distinctions compared to NP-WAS, suggesting a lower concentration of lighter components in the oil from NP-WAS. In stage C, the polymerization of bio-oils into condensed materials, such as resin, alongside the dehydration and condensation of heavy fractions, takes place upon heating. BS-WAS and CS-WAS displayed higher peaks compared to NP-WAS, indicating a more extensive decomposition of heavier fractions in these two oils. The final decomposition stage was broader for NP-WAS and was accompanied by a substantial peak, suggesting a higher production of char during the heating of this bio-oil in the preceding stages.

TGA data also facilitates the estimation of the boiling range of heavy oils, as demonstrated by previous studies [56,57]. The boiling point distribution of the bio crude oils is detailed in Table 7. The weight loss of the samples before 110 °C is consistently less than 2 wt% for all the oils, indicating the effective removal of water during the drying process. A visible shift in the percentage of components with lower boiling points is evident in the oils derived from co-feeds compared to BS, as highlighted in Table 7. Approximately 30–37 % of the bio-oils produced with co-feeds exhibited boiling points lower than 300 °C, a notable increase compared to the 19 % observed for the bio-oil produced with BS alone. This shift implies that the addition of WAS has altered the molecular distribution toward more volatile compounds, emphasizing the impact of co-feedstock composition on the resultant bio-oil characteristics.

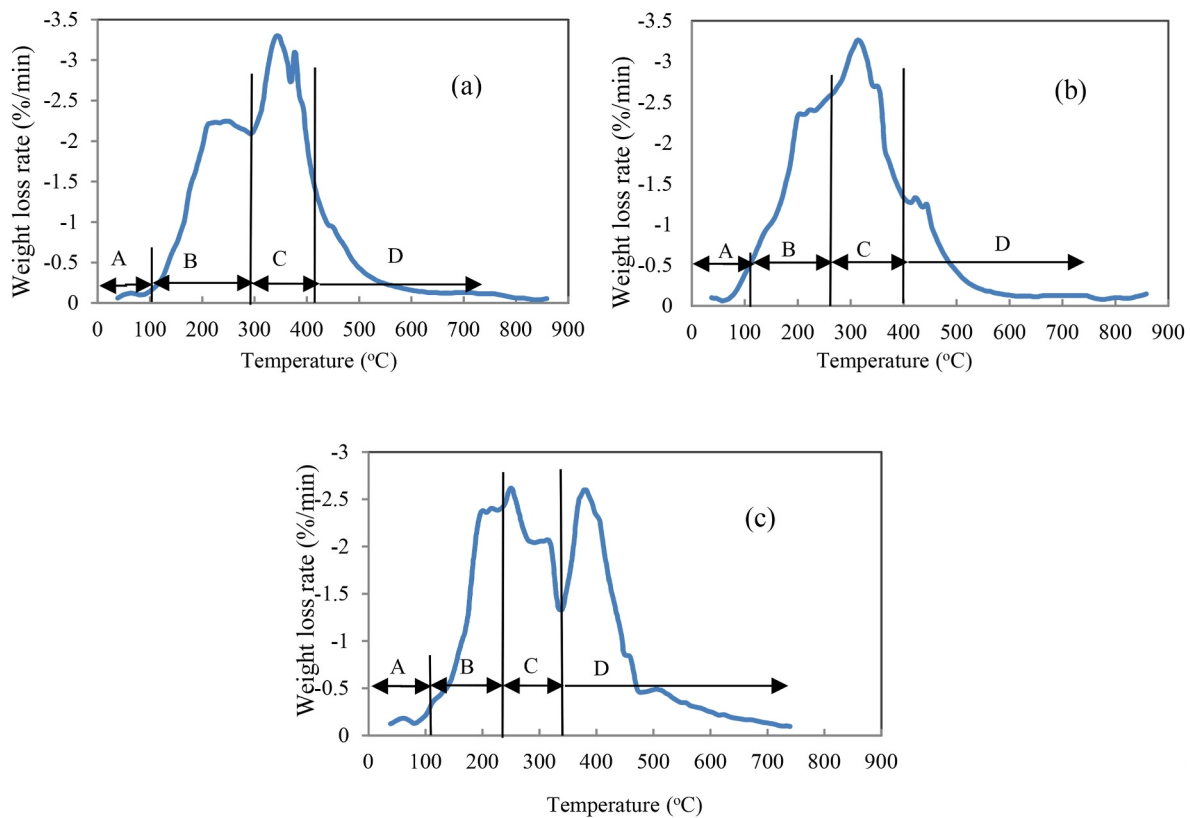


Fig. 6. DGA curves for the bio-oils from BS-WAS (a), CS-WAS (b) and NP-WAS (c).

Table 6

Decomposition start/peak/end temperatures, volatile matter, and fixed carbon of bio-oils.

Oil	Ignition temperature (T_i)	Burnout temperature (T_b)	DTG peak temperature (T_m)	VM (wt%)	FC (wt%)	Ash (wt%)
BS-WAS	168	883	344	73.1	26.8	0.18
CS-WAS	161	880	314	77.4	22.4	0.18
NP-WAS	164	892	250, 380	71.1	28.8	0.08
BS	212	882	367	59.3	40.7	NG
WAS	208	890	284, 419	86.9	12.3	0.71

Table 7

Estimated boiling point distribution of bio-oils (%).

Distillate range (°C)	Bio-oils				
	BS-WAS	CS-WAS	NP-WAS	BS	WAS
40–110	0.78	1.22	1.19	0.13	0.58
110–200	8.03	10.56	9.61	3.29	6.09
200–300	21.82	25.65	23.02	16.41	30.24
300–400	27.88	24.38	20.65	23.97	28.98
400–550	10.79	10.71	11.18	11.12	17.40
550–700	2.19	2.04	3.26	2.97	1.63
700–800	0.87	1.09	1.01	0.88	0.98
800–900	0.60	1.57	1.07	0.56	0.95

3.7. Energy balance

The energy recovery for the HTL of various feedstocks were as follows: 64.81 % for BS-WAS, 57.72 % for CS-WAS, 62.23 % for NP-WAS, 54.47 % for WAS, and 61.51 % for BS. These results underscore the success of HTL in reclaiming over half of the energy present in the feedstock, demonstrating its capability to efficiently convert waste materials into a higher-energy bio-oil. This bio-oil holds significant potential as a renewable energy resource.

The energy recovery of the bio-oil derived from sludge increased

when sludge was co-processed with other lignocellulosic biomass, illustrating the synergistic benefits of adding another waste biomass to the sludge. This enhancement in energy recovery further highlights the promising outcomes of incorporating diverse feedstocks in the HTL process.

4. Conclusion

This study delves into the impact of co-feeding and the utilization of diverse feedstocks on hydrothermal liquefaction. Specifically, three distinct types of lignocellulosic waste biomass were blended with waste activated sludge, undergoing conversion into bio-oil. The analysis of bio-oil yields revealed that the synergistic effects of introducing additional waste biomass depends on the specific type of waste biomass combined with the other one. The bio-oils derived from co-feeds exhibited superior quality characteristics, including lower molecular weights, reduced boiling points, higher volatile matter content, and diminished fixed carbon content compared to bio-oil produced from individual feedstocks. Both by-products generated during this process (biochar and WSP) hold potential applications for energy generation or as fertilizers, as suggested by previous studies, underscoring the multifaceted benefits of hydrothermal liquefaction in the context of waste valorization [58–60].

CRedit authorship contribution statement

Laleh Nazari: Writing – review & editing, Writing – original draft, Validation, Project administration, Methodology, Investigation, Formal analysis, Conceptualization. **Haoyu Wang:** Writing – review & editing. **Madhumita B. Ray:** Writing – review & editing, Validation, Supervision, Resources, Funding acquisition. **Chunbao Xu:** Writing – review & editing, Validation, Supervision, Resources, Project administration, Funding acquisition, Conceptualization.

Acknowledgments

The authors would like to acknowledge the funding from BioFuelNet Canada, Network of Centres of Excellence and from NSERC through the Discovery Grants.

Appendix A. Supplementary data

Supplementary data to this article can be found online at <https://doi.org/10.1016/j.biombioe.2025.107671>.

Data availability

Data will be made available on request.

References

- S.A. Hoang, N. Bolan, A.M.P. Madhubashini, M. Vithanage, V. Perera, H. Wijesekara, H. Wang, P. Srivastava, M.B. Kirkham, B.S. Mickan, J. Rinkebe, K. H.M. Siddique, Treatment processes to eliminate potential environmental hazards and restore agronomic value of sewage sludge: a review, *Environ. Pollut.* 293 (2022), <https://doi.org/10.1016/j.envpol.2021.118564>.
- S. Mohammad Mirsoleimani Azizi, W. Dastyar, M.N.A. Meshref, R. Maal-Bared, B. Ranjan Dhar, Low-temperature thermal hydrolysis for anaerobic digestion facility in wastewater treatment plant with primary sludge fermentation, *Chem. Eng. J.* 426 (2021), <https://doi.org/10.1016/j.cej.2021.130485>.
- J. Ni, L. Qian, Y. Wang, B. Zhang, H. Gu, Y. Hu, Q. Wang, A review on fast hydrothermal liquefaction of biomass, *Fuel* 327 (2022), <https://doi.org/10.1016/j.fuel.2022.125135>.
- B. de Caprariis, P. De Filippis, A. Petruello, M. Scarsella, Hydrothermal liquefaction of biomass: influence of temperature and biomass composition on the bio-oil production, *Fuel* 208 (2017) 618–625, <https://doi.org/10.1016/j.fuel.2017.07.054>.
- D.R. Vardon, B.K. Sharma, J. Scott, G. Yu, Z. Wang, L. Schideman, Y. Zhang, T. J. Strathmann, Chemical properties of biocrude oil from the hydrothermal liquefaction of *Spirulina* algae, swine manure, and digested anaerobic sludge, *Bioresour. Technol.* 102 (2011) 8295–8303.
- Y. Fan, U. Hornung, N. Dahmen, Hydrothermal liquefaction of sewage sludge for biofuel application: a review on fundamentals, current challenges and strategies, *Biomass Bioenergy* 165 (2022), <https://doi.org/10.1016/j.biombioe.2022.106570>.
- W.L. Kranich, A.E. Erarp, Conversion of Sewage Sludge to Oil by Hydroliquefaction, 1984. Cincinnati, OH.
- C. Xu, J. Lancaster, Conversion of secondary pulp/paper sludge powder to liquid oil products for energy recovery by direct liquefaction in hot-compressed water, *Water Res.* 42 (2008) 1571–1582.
- P.M. Molton, A.G. Fassbender, M.D. Brown, STORS: the Sludge-To-Oil Reactor System, 1986. Cincinnati, OH.
- V.K. Tyagi, S.-L. Lo, Sludge: a waste or renewable source for energy and resources recovery, *Renew. Sustain. Energy Rev.* 25 (2013) 708–728.
- K. Malins, V. Kampars, J. Brinks, I. Neibolte, R. Murnieks, R. Kampare, Bio-oil from thermo-chemical hydro-liquefaction of wet sewage sludge, *Bioresour. Technol.* 187 (2015) 23–29, <https://doi.org/10.1016/j.biortech.2015.03.093>.
- H. Huang, X. Yuan, H. Zhu, H. Li, Y. Liu, X. Wang, G. Zeng, Comparative studies of thermochemical liquefaction characteristics of microalgae, lignocellulosic biomass and sewage sludge, *Energy* 56 (2013) 52–60, <https://doi.org/10.1016/j.energy.2013.04.065>.
- R. Obeid, N. Smith, D.M. Lewis, T. Hall, P. van Eyk, A kinetic model for the hydrothermal liquefaction of microalgae, sewage sludge and pine wood with product characterisation of renewable crude, *Chem. Eng. J.* 428 (2021), <https://doi.org/10.1016/j.cej.2021.131228>.
- L. Nazari, Z. Yuan, M.B. Ray, C. Charles Xu, Co-conversion of waste activated sludge and sawdust through hydrothermal liquefaction: optimization of reaction parameters using response surface methodology, *Appl. Energy* 203 (2017) 1–10.
- L. Nazari, Z. Yuan, S. Souzaanchi, M.B. Ray, C. Charles Xu, Hydrothermal liquefaction of woody biomass in hot-compressed water: catalyst screening and comprehensive characterization of bio-crude oils, *Fuel* 162 (2015) 74–83, <https://doi.org/10.1016/j.fuel.2015.08.055>.
- A. Mathanker, D. Pudasainee, A. Kumar, R. Gupta, Hydrothermal liquefaction of lignocellulosic biomass feedstock to produce biofuels: parametric study and products characterization, *Fuel* 271 (2020), <https://doi.org/10.1016/j.fuel.2020.117534>.
- American Public Health Association (APHA), *Standard Methods for the Examination of Water and Wastewater*, twentieth ed., 1960. Washington, DC, USA.
- M. Carrier, A. Loppinet-Serani, D. Denux, J.M. Lasnier, F. Ham-Pichavant, F. Cansell, C. Aymonier, Thermogravimetric analysis as a new method to determine the lignocellulosic composition of biomass, *Biomass Bioenergy* 35 (2011) 298–307, <https://doi.org/10.1016/j.biombioe.2010.08.067>.
- C. Tian, B. Li, Z. Liu, Y. Zhang, H. Lu, Hydrothermal liquefaction for algal bio-refinery: a critical review, *Renew. Sustain. Energy Rev.* 38 (2014) 933–950, <https://doi.org/10.1016/j.rser.2014.07.030>.
- B. Hao, D. Xu, Y. Wei, Y. Diao, L. Yang, L. Fan, Y. Guo, Mathematical models application in optimization of hydrothermal liquefaction of biomass, *Fuel Process. Technol.* 243 (2023), <https://doi.org/10.1016/j.fuproc.2023.107673>.
- B.N. Kuznetsov, S.a. Kuznetsova, V.a. Levdansky, A.V. Levdansky, N.Yu Vasil'eva, N.V. Chesnokov, N.M. Ivanchenko, D. Djakovitch, C. Pinel, Optimized methods for obtaining cellulose and cellulose sulfates from birch wood, *Wood Sci. Technol.* 49 (2015) 825–843, <https://doi.org/10.1007/s00226-015-0723-y>.
- G. Shulga, S. Vitolina, V. Shekels, L. Belkova, G. Cazacu, C. Vasile, L. Nita, Lignin separated from the hydrolyzate of the hydrothermal treatment of birch wood and its surface properties, *Cellul. Chem. Technol.* 46 (2012) 307–318.
- Z. Daud, M. Zainuri, M. Hatta, A. Sari, M. Kassim, H. Awang, A.M. Aripin, V. Education, U. Tun, H. Onn, Analysis the chemical composition and fiber morphology structure of corn stalk, *Aust J Basic Appl Sci* 7 (2013) 401–405.
- J. Flandez, I. González, J.B. Resplandis, N.E. El Mansouri, F. Vilaseca, P. Mutjé, Management of corn stalk waste as reinforcement for polypropylene injection moulded composites, *Bioresources* 7 (2012) 1836–1849.
- H. Chen, Q. Han, R.A. Venditti, H. Jameel, Enzymatic hydrolysis of pretreated newspaper having high lignin content for bioethanol production, *Bioresources* 10 (2015) 4077–4098.
- L. Zhang, P. Champagne, C. Charles Xu, Bio-crude production from secondary pulp/paper-mill sludge and waste newspaper via co-liquefaction in hot-compressed water, *Energy* 36 (2011) 2142–2150, <https://doi.org/10.1016/j.energy.2010.05.029>.
- S.C. Qi, J.I. Hayashi, S. Kudo, L. Zhang, Catalytic hydrogenolysis of kraft lignin to monomers at high yield in alkaline water, *Green Chem.* 19 (2017) 2636–2645, <https://doi.org/10.1039/c7gc01121k>.
- A.A. Shah, K. Sharma, M.S. Haider, S.S. Toor, L.A. Rosendahl, T.H. Pedersen, D. Castello, The role of catalysts in biomass hydrothermal liquefaction and biocrude upgrading, *Processes* 10 (2022), <https://doi.org/10.3390/pr10020207>.
- D. Xu, Y. Wang, G. Lin, S. Guo, S. Wang, Z. Wu, Co-hydrothermal liquefaction of microalgae and sewage sludge in subcritical water: ash effects on bio-oil production, *Renew. Energy* 138 (2019) 1143–1151, <https://doi.org/10.1016/j.renene.2019.02.020>.
- S.S. Toor, L. Rosendahl, A. Rudolf, Hydrothermal liquefaction of biomass: a review of subcritical water technologies, *Energy* 36 (2011) 2328–2342, <https://doi.org/10.1016/j.energy.2011.03.013>.
- C. Jazrawi, P. Biller, A.B. Ross, A. Montoya, T. Maschmeyer, B.S. Haynes, Pilot plant testing of continuous hydrothermal liquefaction of microalgae, *Algal Res.* 2 (2013) 268–277, <https://doi.org/10.1016/j.algal.2013.04.006>.
- B. Bhaskar, A. Sera, A. Muto, Y. Sakata, Hydrothermal upgrading of wood biomass: influence of the addition of K₂CO₃ and cellulose/lignin ratio, *Fuel* 87 (2008) 2236–2242, <https://doi.org/10.1016/j.fuel.2007.10.018>.
- Z. Bi, J. Zhang, E. Peterson, Z. Zhu, C. Xia, Y. Liang, T. Wiltowski, Biocrude from pretreated sorghum bagasse through catalytic hydrothermal liquefaction, *Fuel* 188 (2017) 112–120, <https://doi.org/10.1016/j.fuel.2016.10.039>.
- R. Kaur, B. Biswas, J. Kumar, M.K. Jha, T. Bhaskar, Catalytic hydrothermal liquefaction of castor residue to bio-oil: effect of alkali catalysts and optimization study, *Ind. Crops Prod.* 149 (2020), <https://doi.org/10.1016/j.indcrop.2020.112359>.
- M.K. Jindal, M.K. Jha, Catalytic hydrothermal liquefaction of waste furniture sawdust to bio-oil, *Indian Chem. Eng.* 58 (2016) 157–171, <https://doi.org/10.1080/00194506.2015.1006145>.
- R.B. Carpio, Y. Zhang, C.T. Kuo, W.T. Chen, L.C. Schideman, R. de Leon, Effects of reaction temperature and reaction time on the hydrothermal liquefaction of demineralized wastewater algal biomass, *Bioresour. Technol. Rep.* 14 (2021), <https://doi.org/10.1016/j.biteb.2021.100679>.
- M. Ahmad, A.U. Rajapaksha, J.E. Lim, M. Zhang, N. Bolan, D. Mohan, M. Vithanage, S.S. Lee, Y.S. Ok, Biochar as a sorbent for contaminant management in soil and water: a review, *Chemosphere* 99 (2014) 19–23, <https://doi.org/10.1016/j.chemosphere.2013.10.071>.
- K.W. Jung, K. Kim, T.U. Jeong, K.H. Ahn, Influence of pyrolysis temperature on characteristics and phosphate adsorption capability of biochar derived from waste-marine macroalgae (*Undaria pinnatifida* roots), *Bioresour. Technol.* 200 (2016) 1024–1028, <https://doi.org/10.1016/j.biortech.2015.10.016>.
- X. Wang, W. Zhou, G. Liang, D. Song, X. Zhang, Characteristics of maize biochar with different pyrolysis temperatures and its effects on organic carbon, nitrogen and enzymatic activities after addition to fluvo-aquic soil, *Sci. Total Environ.* 538 (2015) 137–144, <https://doi.org/10.1016/j.scitotenv.2015.08.026>.
- M. Qiu, L. Liu, Q. Ling, Y. Cai, S. Yu, S. Wang, D. Fu, B. Hu, X. Wang, Biochar for the removal of contaminants from soil and water: a review, *Biochar* 4 (2022), <https://doi.org/10.1007/s42773-022-00146-1>.
- R.F. Beims, Y. Hu, H. Shui, C. Charles Xu, Hydrothermal liquefaction of biomass to fuels and value-added chemicals: products applications and challenges to develop

- large-scale operations, *Biomass Bioenergy* 135 (2020), <https://doi.org/10.1016/j.biombioe.2020.105510>.
- [42] B. Zhang, J. Chen, S. Kandasamy, Z. He, Hydrothermal liquefaction of fresh lemon-peel and *Spirulina platensis* blending -operation parameter and biocrude chemistry investigation, *Energy* 193 (2020), <https://doi.org/10.1016/j.energy.2019.116645>.
- [43] L. Qian, B. Zhao, H. Wang, G. Bao, Y. Hu, C. Charles Xu, H. Long, Valorization of the spent catalyst from flue gas denitrogenation by improving bio-oil production from hydrothermal liquefaction of pinewood sawdust, *Fuel* 312 (2022), <https://doi.org/10.1016/j.fuel.2021.122804>.
- [44] H. Jahromi, T. Rahman, P. Roy, S. Adhikari, Hydrotreatment of solvent-extracted biocrude from hydrothermal liquefaction of municipal sewage sludge, *Energy Convers. Manag.* 263 (2022), <https://doi.org/10.1016/j.enconman.2022.115719>.
- [45] S. Dutta, Q. Zhang, Y. Cao, C. Wu, K. Moustakas, S. Zhang, K.H. Wong, D.C. W. Tsang, Catalytic valorisation of various paper wastes into levulinic acid, hydroxymethylfurfural, and furfural: influence of feedstock properties and ferric chloride, *Bioresour. Technol.* 357 (2022), <https://doi.org/10.1016/j.biortech.2022.127376>.
- [46] S. Magalhães, A. Filipe, E. Melro, C. Fernandes, C. Vitorino, L. Alves, A. Romano, M.G. Rasteiro, B. Medronho, Lignin extraction from waste pine sawdust using a biomass derived binary solvent system, *Polymers* 13 (2021), <https://doi.org/10.3390/polym13071090>.
- [47] A. Cemin, F. Ferrarini, M. Poletto, L.R. Bonetto, J. Bortoluz, L. Lemée, R. Guégan, V.I. Esteves, M. Giovanela, Characterization and use of a lignin sample extracted from *Eucalyptus grandis* sawdust for the removal of methylene blue dye, *Int. J. Biol. Macromol.* 170 (2021) 375–389, <https://doi.org/10.1016/j.ijbiomac.2020.12.155>.
- [48] C. Liu, F. Lin, X. Kong, Y. Fan, W. Xu, M. Lei, R. Xiao, Lignin-first biorefinery of corn stalk via zirconium(IV) chloride/sodium hydroxide-catalyzed aerobic oxidation to produce phenolic carbonyls, *Bioresour. Technol.* 354 (2022), <https://doi.org/10.1016/j.biortech.2022.127183>.
- [49] B. Luo, L. Zhou, Z. Tian, Y. He, R. Shu, Hydrogenolysis of cornstalk lignin in supercritical ethanol over N-doped micro-mesoporous biochar supported Ru catalyst, *Fuel Process. Technol.* 231 (2022), <https://doi.org/10.1016/j.fuproc.2022.107218>.
- [50] L. Li, J. Bai, Q. Liu, G. Huang, J. Song, C. Chang, P. Li, S. Pang, Performance research and optimization of the production of high-value nitrogen-containing compounds from tobacco stems via two-step hydrothermal liquefaction, *Biomass Convers Biorefin* (2022), <https://doi.org/10.1007/s13399-022-03006-x>.
- [51] R. Font, a. Fullana, J.a. Conesa, F. Llavador, Analysis of the pyrolysis and combustion of different sewage sludges by TG, *J. Anal. Appl. Pyrolysis* 58–59 (2001) 927–941, [https://doi.org/10.1016/S0165-2370\(00\)00146-7](https://doi.org/10.1016/S0165-2370(00)00146-7).
- [52] A.-B. Hernandez, J.-H. Ferrasse, S. Akkache, N. Roche, Thermochemical conversion of sewage sludge by TGA-FTIR analysis: influence of mineral matter added, *Dry. Technol.* 33 (2015) 1318–1326, <https://doi.org/10.1080/07373937.2015.1036283>.
- [53] S. Li, A. Sanna, J.M. Andresen, Influence of temperature on pyrolysis of recycled organic matter from municipal solid waste using an activated olivine fluidized bed, *Fuel Process. Technol.* 92 (2011) 1776–1782, <https://doi.org/10.1016/j.fuproc.2011.04.026>.
- [54] J. Chen, X. Fan, B. Jiang, L. Mu, P. Yao, H. Yin, X. Song, Pyrolysis of oil-plant wastes in a TGA and a fixed-bed reactor: thermochemical behaviors, kinetics, and products characterization, *Bioresour. Technol.* 192 (2015) 592–602, <https://doi.org/10.1016/j.biortech.2015.05.108>.
- [55] L. Burhenne, J. Messmer, T. Aicher, M.P. Laborie, The effect of the biomass components lignin, cellulose and hemicellulose on TGA and fixed bed pyrolysis, *J. Anal. Appl. Pyrolysis* 101 (2013) 177–184, <https://doi.org/10.1016/j.jaap.2013.01.012>.
- [56] Y. Li, C. Zhu, J. Jiang, Z. Yang, W. Feng, L. Li, Y. Guo, J. Hu, Catalytic hydrothermal liquefaction of *Gracilaria corticata* macroalgae: effects of process parameter on bio-oil up-gradation, *Bioresour. Technol.* 319 (2021), <https://doi.org/10.1016/j.biortech.2020.124163>.
- [57] H.A. Baloch, M.T.H. Siddiqui, S. Nizamuddin, S. Riaz, M. Haris, N.M. Mubarak, G. J. Griffin, M.P. Srinivasan, Effect of solvent on hydro-solvothermal co liquefaction of sugarcane bagasse and polyethylene for bio-oil production in ethanol–water system, *Process Saf. Environ. Protect.* 148 (2021) 1060–1069, <https://doi.org/10.1016/j.psep.2021.02.015>.
- [58] S.P. Munasinghe-Arachchige, I.S.A. Abeysiriwardana-Arachchige, H.M.K. Delanka-Pedige, N. Nirmalakhandan, Biofertilizer recovery from organic solid wastes via hydrothermal liquefaction, *Bioresour. Technol.* 338 (2021), <https://doi.org/10.1016/j.biortech.2021.125497>.
- [59] A.R.K. Gollakota, N. Kishore, S. Gu, A review on hydrothermal liquefaction of biomass, *Renew. Sustain. Energy Rev.* 81 (2018) 1378–1392, <https://doi.org/10.1016/j.rser.2017.05.178>.
- [60] R. Ghadge, N. Nagwani, N. Saxena, S. Dasgupta, A. Sapre, Design and scale-up challenges in hydrothermal liquefaction process for biocrude production and its upgradation, *Energy Convers. Manag.* X 14 (2022), <https://doi.org/10.1016/j.ecmx.2022.100223>.